CHIN. PHYS. LETT. Vol. 38, No. 12 (2021) 124401

Spatiotemporal Modulation of Thermal Emission from Thermal-Hysteresis Vanadium Dioxide for Multiplexing Thermotronics Functionalities

Guanying Xing(邢冠英), Weixian Zhao(赵伟贤), Run Hu(胡润)*, and Xiaobing Luo(罗小兵)

School of Energy and Power Engineering, Huazhong University of Science and Technology, Wuhan 430074, China

(Received 30 September 2021; accepted 3 November 2021; published online 25 November 2021)

Taking heat positively as the information carrier, thermotronics can exempt the long-lasting thermal issue of electronics fundamentally, yet has been faced with the challenging multiplexing integration of diverse functionalities. Here, we demonstrate a spatiotemporal modulation platform to achieve multiplexing thermotronics functionalities based on the thermal-hysteresis vanadium dioxide, including negative-differential thermal emission, thermal diode, thermal memristor, thermal transistor, and beyond. The physics behind the multiplexing thermotronics lies in the thermal hysteresis emission characteristics of the phase-changing vanadium dioxide during the spatiotemporal modulation. The present spatiotemporal modulation is expected to stimulate more exploration on novel functionalities, system integration, and practical applications of thermotronics.

DOI: 10.1088/0256-307X/38/12/124401

As electronic chips are developing toward higher density of power, compactness, and integration, thermal issue, originated from the hardly inevitable Joule effect during the underlying 0–1 Boolean operation, becomes the key bottleneck that limits the working performance and lifetime of electronic chips. Rather than taking heat being "negative", the concept of thermotronics takes heat (either conductive phonon or radiative photon in the quantum level) as the counterpart of electron that plays the role of information carrier, to develop the thermal analogues of electronic components.[1,2] Herein, heat plays a "positive" role, thus the thermal issues are exempted fundamentally, which holds great promise to create a new era of informative world beyond the electronic one. So far, some thermotronics devices have been proposed both theoretically and experimentally, such as thermal diodes,[3] thermal transistors,[4,5] thermal memristors,[6] thermal memories,[7–9] thermal logical gates,[10,11] and thermal computing.[12] However, these attempts are rather independent and dispersive, based on different materials, setups, and configurations, and it is of challenge to systematically integrate the multiple thermotronics functionalities for the ultimate goal of computation with heat. Therefore, a multiplexing platform that can be used to integrate thermotronics functionalities is significantly demanded.

Vanadium dioxide (VO_2), as a typical kind of solid-solid PCMs, undergoes metallic phase and insulating phase reversely within a picosecond time scale around its phase-changing temperature at ∼340 K, resulting in a temperature-dependent emissivity regulation.[13] Below 340 K, VO_2 at insulating phase is less reflective than that at the metallic phase, and thus the corresponding emissivity is much larger, and vice versa. The VO_2 emissivity at the insulating and the metallic phases are $\varepsilon_{\rm i} = 0.79$ and $\varepsilon_{\rm m} = 0.22$, respectively.[6] The emissivity change $\varepsilon_{\rm i}/\varepsilon_{\rm m} = 3.6$ across 340 K is large enough to significantly regulate the radiative heat flux within a small temperature interval. In addition, VO_2 exhibits interesting thermal hysteresis phenomenon, i.e., the phase-changing transition temperatures during heating or cooling circles are different due to the first-order Mott phase transition of VO_2, resulting in the phenomenon that the emissivity curves during heating and cooling are nonoverlapping.[14,15] Due to thermal hysteresis, the surface emissivity of VO_2 is dependent on the derivative of temperature with respect to time:

$$\varepsilon(T) = \varepsilon_h(T)H\Big(\frac{\partial T}{\partial t}\Big) + \varepsilon_c(T)H\Big(-\frac{\partial T}{\partial t}\Big), \quad (1)$$

where $H(\cdots)$ is the Heaviside function, which means when temperature rises (its derivative is larger than zero), $\varepsilon(T) = \varepsilon_h(T)$, and otherwise $\varepsilon(T) = \varepsilon_c(T)$. Further, the emissivity $\varepsilon_h(T)$ and $\varepsilon_c(T)$ can be obtained by fitting to experiments.[6,15] Though the transition temperature, emissivity, and thermal hysteresis can be tuned by doping element,[16,17] inducing interfacial stress,[18] adjusting lattice,[19] and generating defects,[20] we take intrinsic VO_2 for simple demonstration of multiplexing thermotronics functionalities hereinafter.

In this Letter, we demonstrate the multiplex-

Supported by the National Natural Science Foundation of China (Grant No. 52076087), and the Applied Basic Frontier Program of Wuhan City (Grant No. 2020010601012197).

*Corresponding author. Email: hurun@hust.edu.cn

ing thermotronics functionalities through spatiotemporal modulation of the thermal emission from VO_2 plates, including negative-differential thermal emission, thermal diodes, thermal memristors, thermal transistors, and beyond. The key characteristic of each thermotronics functionality is simply introduced firstly and then followed by detailed discussions of the present spatiotemporal modulation platform. The present study is expected to open a new avenue in development of thermotronics, thermal computing, and thermal management.

Negative-Differential Thermal Emission (NDTE). Over centuries, there appears a consensus that hotter objects emit more power, i.e., the differential thermal emission $\partial q/\partial T$ is always positive. The physical premise of such a consensus is that the surface emissivity is nearly a constant, i.e., the differential emissivity $\partial\varepsilon(T)/\partial T$ approaches zero. Such a premise may be correct for most materials, but no longer holds for PCMs whose optical properties are strongly changed with temperature, thus enabling the NDTE functionality.[21,22] For this end, we derive the differential of q as

$$\frac{\partial q}{\partial T} = 4\sigma\varepsilon(T)T^3 + \sigma T^4\frac{\partial\varepsilon(T)}{\partial T}, \tag{2}$$

where σ is the Stefan–Boltzmann constant and T is the temperature. To achieve NDTE in the far field, Eq. (2) must be less than zero, and thus the temperature coefficient of emissivity (TCE), defined as $\text{TCE} = 1/\varepsilon(T)|\partial\varepsilon(T)/\partial T|$ must be larger than $4/T$, and the derivative of emissivity with respect to temperature $\partial\varepsilon(T)/\partial T$ must be negative.[22]

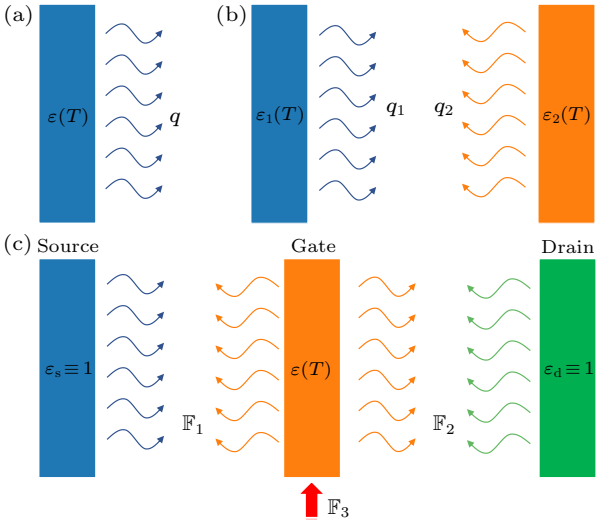

Fig. 1. Schematic for thermotronics setups. (a) Negative-differential thermal emission (NDTE). (b) Thermal diode or thermal memristor. (c) Thermal transistor.

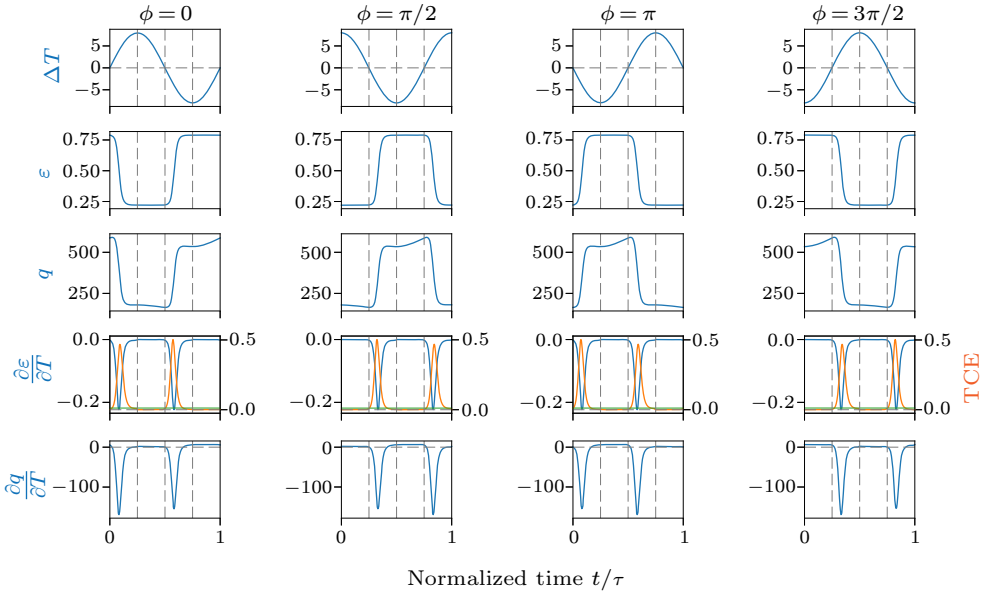

Fig. 2. Spatiotemporal modulation for negative-differential thermal emission (NDTE). A VO_2 plate with a sinusoidal temperature variation $\Delta T = 8\sin(2\pi t/\tau + \phi)$ with phases $\phi = 0$, $\pi/2$, π, $3\pi/2$, respectively.

To demonstrate the NDTE achieved by spatiotemporal modulation, we apply a spatial and temporal temperature variation $\Delta T(x,t)$ to modulate the temperature of VO_2 plate as $T(x,t) = T_0 + \Delta T(x,t)$ with respect to the reference temperature T_0, which is set as the mean temperature of $T_{0,\text{h}}$ (phase transition temperature in the heating curve) and $T_{0,\text{c}}$ (phase transition temperature in the cooling curve), as shown in Fig. 1(a). We consider the $\Delta T(x,t)$ to be a spatiotemporal function that varies sinusoidally with time t and travels along the x direction at a speed v_0 as $\Delta T(x,t) = \theta\sin[2\pi(x + v_0 t)/d] = \theta\sin(2\pi t/\tau + \phi)$.[23] Here, θ is the amplitude of sinusoidal ΔT that should be large enough (>8 K) to cover the thermal hysteresis loop of VO_2 after one period τ; d is the spatial wavelength of the sinusoidal ΔT, and the spatial phase

$2\pi x/d$ is denoted as ϕ for short hereinafter. Such a spatiotemporally modulated temperature variation can be experimentally achieved with electrical heating or cooling unit, whereas the electrical heating or cooling frequency should be modulated to make sure that the period τ is longer than the thermalization time of VO_2.[6] After such a setup, the corresponding time-dependent ΔT, ε, q, $\partial\varepsilon/\partial T$, and $\partial q/\partial T$ with four spatial phases $\phi = 0$, $\pi/2$, π, $3\pi/2$ are shown in Fig. 2. It is seen that as ΔT is spatiotemporally modulated periodically with respect to phase and time, all the quantities of interest are also spatiotemporally modulated periodically. Let us take the phase $\phi = 0$ as an example to explain detailedly. When the temperature rises across the heating phase transition temperature $T_{0,\mathrm{h}}$ in the first quarter period, the emissivity drops significantly from ε_i to ε_m due to the phase transition from insulating to metallic, resulting in the similar trend of emitted power q. When the temperature drops in the second quarter period, the emissivity almost maintains the same as ε_m due to the thermal hysteresis behavior as the temperature is still above the cooling phase transition temperature $T_{0,\mathrm{c}}$. However, the emitted power continues decreasing due to the drop of temperature according to the Stefan–Boltzmann law. When the temperature continues dropping across the $T_{0,\mathrm{c}}$ in the third quarter period, the emissivity increases from ε_m to ε_i due to the reversed phase transition, resulting in the abrupt increase of emitted power q. When the temperature begins to increase before reaching $T_{0,\mathrm{h}}$ in the fourth quarter period, the emissivity almost maintains the same as ε_i and the emitted power continue increasing due to the increase of temperature. This is the behaviors of emissivity and emitted power of VO_2 with the absence of spatial phase in the complete period and thermal hysteresis loop, based on which we can easily obtain the $\partial\varepsilon/\partial T$ and $\partial q/\partial T$ in Fig. 2. The abrupt changes of emissivity and emitted power in the first and third quarter periods give rise to the corresponding sudden change of the derivative simultaneously. The TCE curve is also plotted in Fig. 2, which is larger than $4/T$ in the corresponding periods, thus ensuring the occurrence of NDTE.[22] Such detailed analyses can also be implemented for other spatial phase ϕ. From Fig. 2, we can see that the NDTE occurs and can be spatiotemporally modulated.

Thermal Diode. A thermal diode, also known as thermal rectifier, allows heat transfer between two terminals in one direction but blocks heat transfer in the opposite direction, which has been proposed and demonstrated in the conductive,[3,24–26] convective,[27] and radiative[28–30] regimes. The key characteristic lies in the nonlinear thermal properties, either conductivity or emissivity, which rectifies the heat flux when interchanging the high- and low-temperature terminals. Here we show that thermal diode can also be achieved via spatiotemporal modulation of VO_2. Assume that a VO_2 plate maintained at $T_1(x,t) = T_0 + \Delta T_1(x,t)$ is separated to a black-body plate with $T_2(x,t) = T_0 + \Delta T_2(x,t)$, where $\Delta T_1 = 8\sin(2\pi t/\tau + \phi_1)$ and $\Delta T_2 = 16\sin(2\pi t/\tau)$, as shown in Fig. 1(b). The forward and backward heat fluxes exchanged between the two plates with the same area read $q_\mathrm{F} = \sigma\varepsilon_\mathrm{F}(T)(T_\mathrm{H}^4 - T_\mathrm{L}^4)$, and $q_\mathrm{B} = \sigma\varepsilon_\mathrm{B}(T)(T_\mathrm{H}^4 - T_\mathrm{L}^4)$, where T_H and T_L are the high and low temperatures of the two terminals, and thus the rectification factor R could be defined as[31]

$$R = \frac{|q_\mathrm{F} - q_\mathrm{B}|}{\max(q_\mathrm{F}, q_\mathrm{B})} = \frac{|\varepsilon_\mathrm{F} - \varepsilon_\mathrm{B}|}{\max(\varepsilon_\mathrm{F}, \varepsilon_\mathrm{B})}, \tag{3}$$

where $\varepsilon_\mathrm{F} = 1/[1/\varepsilon_1(T_1) + 1/\varepsilon_2(T_2) - 1]$, $\varepsilon_\mathrm{B} = 1/[1/\varepsilon_1(T_2) + 1/\varepsilon_2(T_1) - 1]$; $\varepsilon_\mathrm{F} = \varepsilon_1(T_1)$ and $\varepsilon_\mathrm{B} = \varepsilon_1(T_2)$ since the black-body emissivity ε_2 is equal to unity and independent of temperature.

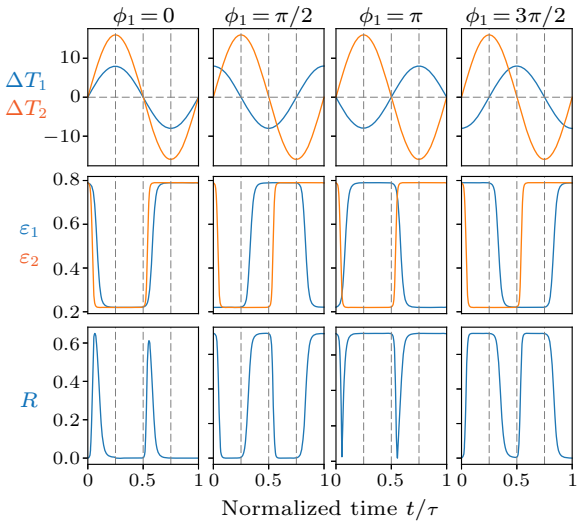

Fig. 3. Spatiotemporal modulation for thermal diode. The separated two VO_2 plates with sinusoidal temperature variations: $\Delta T_1 = 8\sin(2\pi t/\tau + \phi_1)$ and $\Delta T_2 = 16\sin(2\pi t/\tau)$. Each column denotes the corresponding curves with the same ϕ_1.

After such a setup, the corresponding time-dependent ΔT_1, ΔT_2, $\varepsilon_1(T_1)$, $\varepsilon_1(T_2)$, and R with four spatial phases $\phi_1 = 0$, $\pi/2$, π, $3\pi/2$ are shown in Fig. 3. It is seen that as time elapses, ΔT is spatiotemporally modulated periodically with respect to phase and time, and the emissivity and rectification ratio are also spatiotemporally modulated. As temperature changes sinusoidally in one period, the VO_2 undergoes a full loop of thermal hysteresis, as explained above. Let us take the phase $\phi_1 = 0$ as an example to explain the details. In the first and third quarter periods, both $\varepsilon_1(T_1)$ and $\varepsilon_1(T_2)$ vary significantly, while R increases sharply from zero to 0.65 and then drops back to zero. This is caused by the sharp change of emissivity of the

two VO_2 plates during the phase-changing transition. Since the amplitude of ΔT_2 is larger, its emissivity changes more sharply. In the second and fourth quarter periods, both ε_1 and ε_2 become the same as those in the metallic phase, thus giving rise to the zero R according to Eq. (3). From Fig. 3, it is seen that R is spatiotemporally modulated with respect to time and phase. When the spatial phase is $\phi_1 = \pi$, we can realize that $\varepsilon_1(T_1)$ and $\varepsilon_1(T_2)$ are at different phases and R maintains as large as $(\varepsilon_{\rm i}-\varepsilon_{\rm m})/\varepsilon_{\rm i} = 0.72$. We further find that the spatial phase difference is determinative: when the phase difference $|\phi_1 - \phi_2|$ is zero, R is small at most of the time, while phase difference $|\phi_1 - \phi_2|$ is π, R is large at most of the time, as demonstrated in Fig. 4.

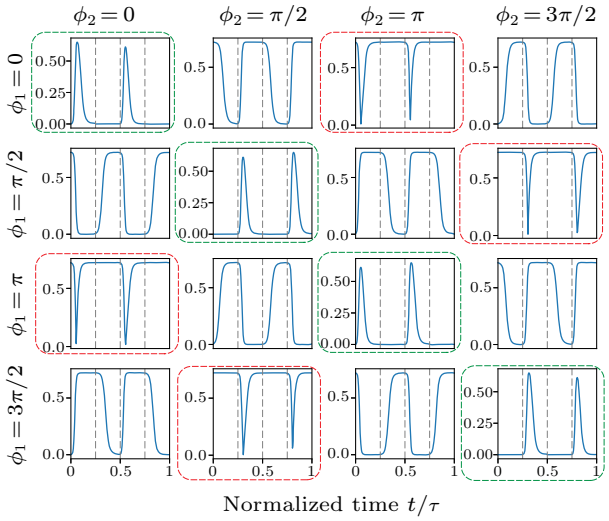

Fig. 4. Spatiotemporal modulation for thermal diode. The separated two VO_2 plates with sinusoidal temperature variations: $\Delta T_1 = 8\sin(2\pi t/\tau + \phi_1)$ and $\Delta T_2 = 16\sin(2\pi t/\tau + \phi_2)$. Each column and row denote the corresponding curves with the same ϕ_1 and ϕ_2, respectively.

Thermal Memristor. An electrical memristor, as the fourth fundamental circuit element accompanied with resistor, capacitor, and inductor, is expected to play an important role in future electronic industry.[32] The key characteristic is the nonlinear hysteresis effect that induces a Lissajous I–V curve across the zero point. Similarly, a thermal memristor, possessing a pinched Lissajous q–T curve, is expected to contribute to the area of thermotronics significantly.[6] Here we show that thermal memristor functionality can also be achieved via the spatiotemporal modulation of VO_2. Assume that a VO_2 plate maintained at $T_1(x,t) = T_0 + \Delta T_1(x,t)$ is separated to a black-body plate with $T_2(x,t) = T_0 + \Delta T_2(x,t)$ respectively, where $\Delta T_1 = 8\sin(2\pi t/\tau + \phi_1)$ and $\Delta T_2 = 16\sin(2\pi t/\tau + \phi_2)$, as shown in Fig. 1(b). For simplicity, here we maintain the reference temperature T_0 as the same. The heat flux exchanged between the two plates is given as $q = \sigma\varepsilon(T)(T_1(x,t)^4 - T_2(x,t)^4)$, where the effective emissivity could be simplified to $\varepsilon(T) = 1/[1/\varepsilon_1(T_1) + 1/\varepsilon_2(T_2) - 1] = \varepsilon_1(T_1)$ as the black-body emissivity $\varepsilon_2 \equiv 1$. Since the temperature difference $\Delta T = \Delta T_1 - \Delta T_2$ is periodically modulated, the emissivity and heat flux are also periodically modulated, generating a closed loop with the time-dependent evolution trajectory. The effective thermal resistance $M = \Delta T/q$ represents the history of the input temperature difference, which can be denoted as the thermal memory resistance, analogous to the Lissajous I–V curve of the electrical memristor.

After such a setup, the corresponding q–ΔT and M–ΔT curves are plotted in Fig. 5, where the left and right y-axes are q and M, respectively, in each subplot. To denote the trajectory of time evolution, we use four colors (blue, orange, green, and purple in series) to represent the successive four quarter periods, respectively. The q–ΔT curves will cross the zero point no matter how we modulate the spatial phases ϕ_1 and ϕ_2, which is easy to understand that, when the temperature difference vanishes, the net heat flux between the two plates becomes zero. All the q–ΔT curves include four parts of behaviors: two linear and two nonlinear behaviors with respect to the quarter period. The two linear behaviors reflect the proportional dependence of heat flux q and temperature difference ΔT as $q = \Delta T/M$, where the slope M^{-1} is a constant due to the absence of VO_2 phase transitions. In contrast, the two nonlinear behaviors correspond to the VO_2 phase transition where the emissivity abruptly changes due to the thermal hysteresis characteristics. Such quasi- and non-linear behaviors can also be observed in the M–ΔT curves, corresponding to the absence and presence of VO_2 phase transition at the same quarter period. The high and low quasi-linear behaviors can be used to define the on-off states of the thermal memristor. It is also seen that both q–ΔT and M–ΔT loops are influenced by the phase difference $\Delta\phi = \phi_1 - \phi_2$. When the phase difference $\Delta\phi$ equals zero, both q–ΔT and M–ΔT curves are similar respectively though their quarter period contributions are different. When the phase difference $\Delta\phi$ equals $\pi/2$ and $-3\pi/2$, the shapes of q–ΔT and M–ΔT loops are different from others. The nonlinear behaviors of q–ΔT loops vanish and the width of M–ΔT loops is largest, offering superior thermal memristor characteristic like the rectangular hysteresis materials.[33]

Thermal Transistor. The electrical transistor, composed of a source, a drain, and a gate, is the cornerstone for establishing the modern electrical and informative world.[34] The key characteristic is that a small voltage applied in the gate can be used to amplify or switch electrical signals between the drain and the source. Similarly, a thermal transistor, which can be used to tune the heat flux with a small energy input, has also been proposed via phonons[2,35] and near-field photons.[4,5]

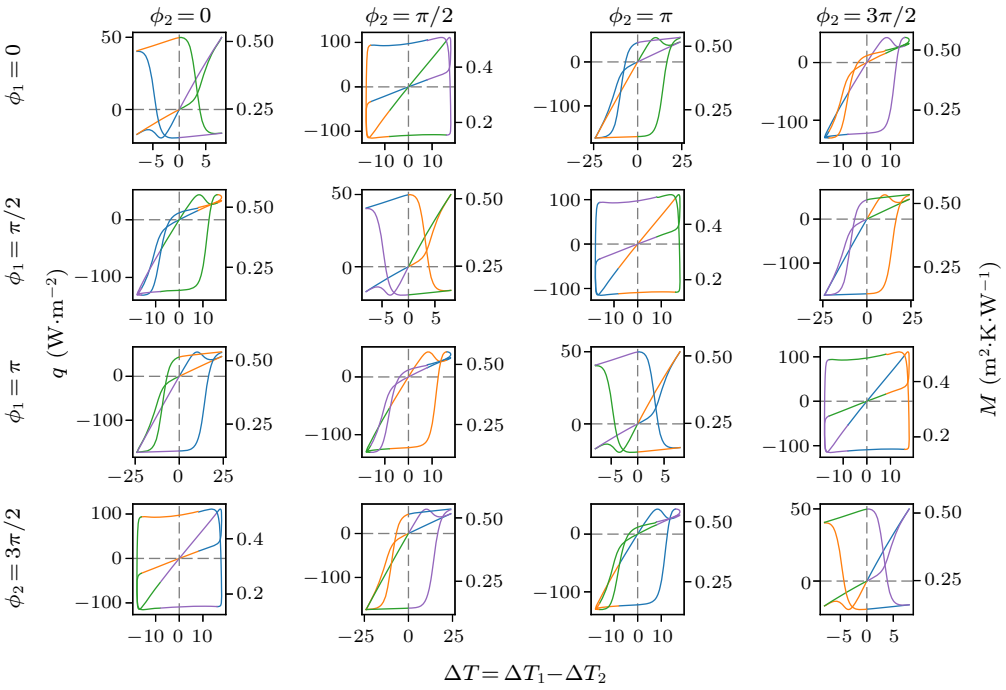

Fig. 5. Spatiotemporal modulation for thermal memristor. The separated VO_2 plate and black-body plate with sinusoidal temperature variations: $\Delta T_1 = 8\sin(2\pi t/\tau + \phi_1)$ and $\Delta T_2 = 16\sin(2\pi t/\tau + \phi_2)$, respectively. Each column and each row denote the Lissajous q–ΔT and M–ΔT curves with the same ϕ_1 and the same ϕ_2, respectively.

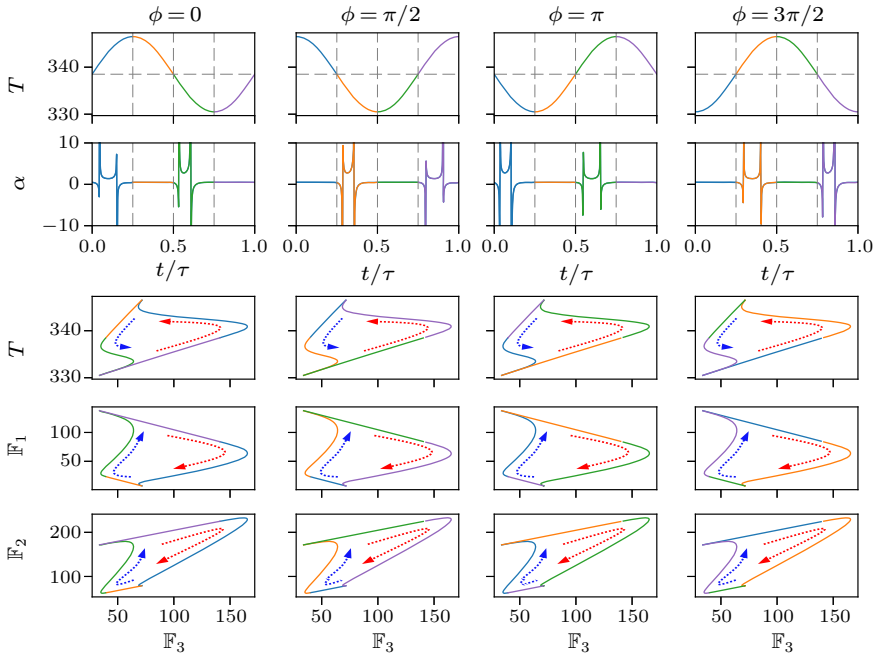

Fig. 6. Spatiotemporal modulation for thermal transistor. A VO_2 plate with sinusoidal temperature variations: $\Delta T = 8\sin(2\pi t/\tau + \phi)$ is put in between a black-body source thermostat (T_s) and a black-body drain thermostat (T_d). Each column denotes the corresponding curves with the same ϕ. The red and blue dashed arrows denote the heating and cooling process in one period.

Here we show that thermal transistor functionality can also be achieved via the spatiotemporal modulation of VO_2. Assume that a VO_2 gate plate maintained at $T(x,t) = T_0 + \Delta T(x,t) = T_0 + 8\sin(2\pi t/\tau + \phi)$ is placed between two separated black-body plates at source thermostat of $T_s = 350\,\mathrm{K}$ and drain thermostat of $T_d = 300\,\mathrm{K}$, as shown in Fig. 1(c). The heat flux between the source (drain) and the gate reads $\mathbb{F}_1 = \sigma\varepsilon(T)(T_s^4 - T^4)$ and $\mathbb{F}_2 = \sigma\varepsilon(T)(T^4 - T_d^4)$. From the principle of energy conservation, the input heat flux to the gate is $\mathbb{F}_3 = \mathbb{F}_2 - \mathbb{F}_1 = \sigma\varepsilon(T)(2T^4 - T_s^4 - T_d^4)$. The equilibrium temperature T_g of the gate can be

obtained by setting $\mathbb{F}_3 = 0$. To quantify the thermal transistor characteristics, we define the heat flux amplification factor as[5]

$$\alpha = \frac{\partial \mathbb{F}_2}{\partial \mathbb{F}_3} = \frac{\frac{d\varepsilon(T)}{dT}(T^4 - T_{\rm d}^4) + 4\varepsilon(T)T^3}{\frac{d\varepsilon(T)}{dT}(2T^4 - T_{\rm s}^4 - T_{\rm d}^4) + 8\varepsilon(T)T^3}. \quad (4)$$

From Eq. (4), when $d\varepsilon(T)/dT$ is zero, i.e., the emissivity is constant, the amplification factor $\alpha = 0.5$. When the denominator $\partial\mathbb{F}_3/\partial T$ vanishes, the amplification factor α diverges, implying that a small change on $\mathbb{F}_3$ will generate a relatively large change on T. After such a setup, the corresponding ΔT, α, the interdependence of three heat fluxes ($\mathbb{F}_1$, $\mathbb{F}_2$, $\mathbb{F}_3$), with four spatial phases $\phi = 0, \pi/2, \pi, 3\pi/2$ are plotted in Fig. 6. It is seen that as ΔT is spatiotemporally modulated periodically with respect to phase and time, all the quantities of interest are also spatiotemporally modulated periodically. The interdependence of T–$\mathbb{F}_3$, $\mathbb{F}_1$–$\mathbb{F}_3$, $\mathbb{F}_2$–$\mathbb{F}_3$ forms asymmetric loops, which include two linear and two nonlinear behaviors of VO_2. When the spatial phase changes, the loops maintain the same shape although the contribution of each quarter period varies. Let us take the phase $\phi = 0$ as an example to explain the details. When temperature variation is sinusoidally modulated, the corresponding emissivity ε and its derivative $\partial\varepsilon/\partial T$ can be found in Fig. 2. At the second and fourth quarter periods, no phase transition happens and $\partial\varepsilon/\partial T$ vanishes, thereby the corresponding α equals 0.5. At the first and third quarter periods, the NDTE happens and amplification factor α diverges when $\partial\mathbb{F}_3/\partial T = 0$, which corresponds to the critical $\mathbb{F}_3$. There exists two critical $\mathbb{F}_3$ in the first and third quarter periods, when insulating-to-metallic and metallic-to-insulating phase transitions occur in VO_2. The critical $\mathbb{F}_3$ implies a large temperature jump with $\partial T/\partial\mathbb{F}_3 = \infty$ locally, which signifies that a small change of applied heat flux $\mathbb{F}_3$ will induce a large change of VO_2 temperature. The same critical $\mathbb{F}_3$ can also be observed when $\partial\mathbb{F}_3/\partial\mathbb{F}_1 = 0$ and $\partial\mathbb{F}_3/\partial\mathbb{F}_2 = 0$ as the change of $\mathbb{F}_2$ and $\mathbb{F}_2$ should be balanced during heating and cooling processes due to the thermal hysteresis of VO_2. Similarly, the critical $\mathbb{F}_3$ also corresponds to a large heat flux jump with $\partial\mathbb{F}_2/\partial\mathbb{F}_3 = \infty$, which is the figure of merit of a thermal transistor that a small change of applied heat flux will induce a large heat flux change across the thermal transistor. With thermal transistor functionality, the thermal switching, modulation, and amplification can also be obtained similarly.[4]

In conclusion, based on the thermal-hysteresis vanadium dioxide, a spatiotemporal modulation platform to achieve multiplexing thermotronics functionalities, like negative-differential thermal emission, thermal diode, thermal memristor, and thermal transistor, is demonstrated. The characteristics of these four thermal functionalities are introduced and the factors affecting their performance are investigated. The mechanism can be attributed to the intrinsic thermal hysteresis emission characteristics of vanadium dioxide during the spatiotemporal modulation of temperature. The present study is expected to inspire development of thermotronics, thermal computing, thermal management, and beyond.

References

[1] Ben-Abdallah P and Biehs S A 2017 *Z. Naturforsch. A* **72** 151
[2] Li N, Ren J, Wang L, Zhang G, Hanggi P and Li B 2012 *Rev. Mod. Phys.* **84** 1045
[3] Kang H, Yang F and Urban J J 2018 *Phys. Rev. Appl.* **10** 024034
[4] Ben-Abdallah P and Biehs S A 2014 *Phys. Rev. Lett.* **112** 044301
[5] Ordonez-Miranda J, Ezzahri Y, Drevillon J and Joulain K 2016 *Phys. Rev. Appl.* **6** 054003
[6] Ordonez-Miranda J, Ezzahri Y, Tiburcio-Moreno J A, Joulain K and Drevillon J 2019 *Phys. Rev. Lett.* **123** 025901
[7] Wang L and Li B W 2008 *Phys. Rev. Lett.* **101** 267203
[8] Hu R, Huang S, Wang M, Zhou L, Peng X and Luo X 2018 *Phys. Rev. Appl.* **10** 054032
[9] Kubytskyi V, Biehs S A and Ben-Abdallah P 2014 *Phys. Rev. Lett.* **113** 074301
[10] Paolucci F, Marchegiani G, Strambini E and Giazotto F 2018 *Phys. Rev. Appl.* **10** 024003
[11] Wang L and Li B 2007 *Phys. Rev. Lett.* **99** 177208
[12] Loke D, Skelton J M, Chong T C and Elliott S R 2016 *ACS Appl. Mater. Interfaces* **8** 34530
[13] Kats M A, Blanchard R, Zhang S, Genevet P, Ko C, Ramanathan S and Capasso F 2013 *Phys. Rev. X* **3** 041004
[14] Gomez-Heredia C L, Ramirez-Rincon J A, Ordonez-Miranda J, Ares O, Alvarado-Gil J J, Champeaux C, Dumas-Bouchiat F, Ezzahri Y and Joulain K 2018 *Sci. Rep.* **8** 8479
[15] Qazilbash M M, Brehm M, Chae B G, Ho P C, Andreev G O, Kim B J, Yun S J, Balatsky A V, Maple M B, Keilmann F, Kim H T, Basov D N 2007 *Science* **318** 1750
[16] Tang K, Wang X, Dong K, Li Y, Li J, Sun B, Zhang X, Dames C, Qiu C, Yao J and Wu J 2020 *Adv. Mater.* **32** 1907071
[17] Chen S, Liu J, Wang L, Luo H and Gao Y 2014 *J. Phys. Chem. C* **118** 18938
[18] Petit C, Frigerio J M and Goldmann M 1999 *J. Phys. Condens. Matter* **11** 3259
[19] Liang Y G, Lee S, Yu H S, Zhang H R, Liang Y J, Zavalij P Y, Chen X, James R D, Bendersky L A, Davydov A V, Zhang X H and Takeuchi I 2020 *Nat. Commun.* **11** 3539
[20] Du J, Gao Y F, Luo H J, Kang L T, Zhang Z T, Chen Z and Cao C X 2011 *Solar Energ. Mater. Solar C* **95** 469
[21] Shahsafi A, Roney P, Zhou Y, Zhang Z, Xiao Y, Wan C, Wambold R, Salman J, Yu Z, Li J, Sadowski J T, Comin R, Ramanathan S and Kats M A 2019 *Proc. Natl. Acad. Sci. USA* **116** 26402
[22] Bierman D M, Lenert A, Kats M A, Zhou Y, Zhang S, De La O M, Ramanathan S, Capasso F and Wang E N 2018 *Phys. Rev. Appl.* **10** 021001
[23] Torrent D, Poncelet O and Batsale J C 2018 *Phys. Rev. Lett.* **120** 125501
[24] Wang Y, Vallabhaneni Y, Hu J, Qiu B, Chen Y P and Ruan X 2014 *Nano Lett.* **14** 592

[25] Cottrill A L, Wang S, Liu A T, Wang W J and Strano M S 2018 *Adv. Energy Mater.* **8** 1702692
[26] Cottrill A L and Strano M S 2015 *Adv. Energy Mater.* **5** 1500921
[27] Gaddam P R, Huxtable S T and Ducker W A 2017 *Int. J. Heat Mass Transfer* **106** 741
[28] Otey C R, Lau W T and Fan S 2010 *Phys. Rev. Lett.* **104** 154301
[29] Fiorino A, Thompson D, Zhu L, Mittapally R, Biehs S A, Bezencenet O, El-Bondry N, Bansropun S, Ben-Abdallah P, Meyhofer E and Reddy P 2018 *ACS Nano* **12** 5774
[30] Jia S, Fu Y, Su Y and Ma Y 2018 *Opt. Lett.* **43** 5619
[31] Kasali S O, Ordonez-Miranda J and Joulain K 2020 *Int. J. Heat. Mass Transfer* **154** 119739
[32] Strukov D B, Snider G S, Stewart D R and Williams R S 2008 *Nature* **453** 80
[33] Magnus F, Wood B, Moore J, Morrison K, Perkins G, Fyson J, Wiltshire M C K, Caplin D, Cohen L F and Pendry J B 2008 *Nat. Mater.* **7** 295
[34] Lu H and Seabaugh A 2014 *IEEE J. Electron. Devices Soc.* **2** 44
[35] Li B, Wang L and Casati G 2006 *Appl. Phys. Lett.* **88** 143501